The final publication is available at Springer via http://dx.doi.org/10.1023/A:1004239409813

Deviations Induced by Tool Sharpening in the Profile of Three Screw Pump Rotors

GIOVANNI MIMMI[1] and PAOLO PENNACCHI[2]
[1]Università degli studi di Pavia, Dipartimento di Meccanica Strutturale, Via Ferrata 1, I-27100 Pavia, Italy
[2]Politecnico di Milano, Dipartimento di Meccanica, Piazza Leonardo da Vinci 32, I-20133 Milano, Italy

Abstract. Three screw pumps represent an important family of positive displacement rotary pumps. They are quite easy to construct, even if the use of a shaped milling cutter for the rotor machining can cause some problems when the tool is not new. In fact the sharpening of the tool modifies the total geometry of the milling cutter by reducing its diameter. The shape of the single cutter does not change, but the cutter radial position is shifted towards the tool center. This causes deviations in the profile cut and the screws consequently need a long breaking-in. In this paper the problem is analyzed from a quantitative point of view, using a method that allows us to determine the machining error as a function of the tool geometry variation. Moreover some alternative solutions to this problem are suggested.

Sommario. Le pompe a tre viti rappresentano un'importante famiglia di pompe volumetriche rotative. La loro realizzazione è abbastanza semplice, anche se l'uso di frese di forma per la lavorazione dei rotori può causare alcuni problemi quando l'utensile non sia nuovo. Infatti la riaffilatura dell'utensile modifica la geometria complessiva della fresa, riducendone il diametro. La forma dei singoli taglienti resta immutata, ma la posizione radiale del tagliente risulta spostata verso il centro dell'utensile. Tale fatto determina degli scostamenti nel taglio dei profili e di conseguenza le viti realizzate richiedono un rodaggio prolungato. Nel presente lavoro si analizza il problema dal punto di vista quantitativo, utilizzando una metodologia che permette di valutare l'entità dell'errore di lavorazione commesso in funzione della variazione della geometria dell'utensile. Inoltre vengono suggerite alcune soluzioni possibili a questo problema.

Key words: Kinematics of mechanisms, Computational techniques, Machining.

Nomenclature

A - definition set of the parameters of the surface of revolution;
g - equation of meshing for the tools;
L - rotation transformation matrix;
v - velocity;
δ - radial shift due to tool sharpening;
ε - machining error;
Θ - solution locus of the tool equation of meshing;
ρ - radial distance of a point of a contact line from the rotor rotation axis;
$\boldsymbol{\omega}$ - angular velocity vector;
ω - angular velocity vector component.

1. Introduction

Even if the name *screw pump* defines many types of positive displacement pumps, which have different numbers of rotors, in this paper we will consider only the three screw type, already studied by the authors in [1] and [2].

The pump here examined is quite important from the commercial point of view, since it represents about 15% of the total number of the pieces of positive displacement rotary pumps sold in the world. There are many applications for screw pumps and some characteristic fields are:

– petroliferous: pumping of high viscosity crude oils and bitumens;
– chemical: transport of liquid-gaseous mixtures and paints;
– food industry: pumping of vegetable oils, thick liquids, syrups, molasses, pastes, fats, sauces and mashes;
– driving devices: oleodynamical devices on machines, shears and lifts;
– lubrication: force feed lubrication for motors, reduction units and rolling mills;
– navy: pumping of fuel and oil.

These pumps may work both externally in relation to the fluid or submerged. The latter situation presents advantages for noise reduction. The working fluids should have a minimal lubricating capability and should be free of abrasive particles. The flow rates depend on the dimensions and are in the range between 3 and 11500 l/min, while the delivery pressure can reach a maximum value of 250 bar. The average noise level is between 52 and 75 dB(A) at 2900 r.p.m.

2. The Screw Rotors and Their Machining

The main constitutive parts of the pumps are the following: a steel central screw rotor connected to the driving shaft, two steel idler screw rotors driven by the central screw rotor, and an aluminum alloy case that can have a pressed-in liner for

the rotor housing. The two types of screw rotors present in the pump are different since the central rotor presents two helical worms, while the idler has two helical vanes.

However the machining technology is the same for both rotors: the rotors are usually cut from a solid piece, by shaped milling cutters. The workpiece has the feeding motion and performs a screw motion, while the milling cutter has the cut motion.

The milling cutters normally used are solid, in high speed steel and have the following characteristics given by ISO 3855 specification [3]:

- slab milling both on the bottom of the rotors and flanks of the worms and the vanes;
- straight teeth, eccentric relieved teeth, side milling cutter and equally spaced teeth;
- usually the cutters are 12, the top rake is 6° and the bottom rake varies from 6° to 12°.

The choice of eccentric relieved teeth, with the top shaped following a logarithmic spiral, or Archimedes' spiral in approximate executions, allows for an easy sharpening that is done on the face of the cutter, which leaves the bottom rake and also the shape of the cutter [4] [5] constant.

This apparently positive characteristic actually introduces some deviations in the machining, which will be calculated in this paper. In fact it will be shown that the sharpening, which reduces the diameter of the milling cutter, even if it does not change the shape of the cutter, makes this shape inexact for the cut of kinematically correct screw rotors.

Now it would be useful to analyze the scheme of the method introduced, which is reported in figure 1.

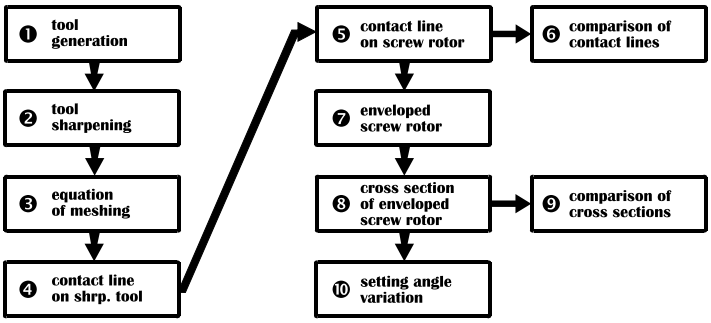

Figure 1 - Scheme of the method.

For the determination of the cutter profile (❶ in figure 1), we refer to a previous paper [2], where a mathematical representation of the tool is given. Here we introduce the tool diameter reduction due to the sharpening and the new contact line on the workpiece is determined by inversion of the procedure introduced in [2]. This new contact line envelops a new screw rotor, which is generally different from the correct screw. The comparison of the two contact lines related to a new milling cutter and a sharpened one respectively, allows us to define the deviations in the machining (❻ in figure 1), while the comparison of the cross sections of the screw rotors allows us to better evaluate the differences (❾ in figure 1).

The analysis ends with a verification of whether a modification of the machining parameters can obviate the machining errors introduced by the tool sharpening (❿ in figure 1).

2.1. Reference Systems and Coordinate Transformation

In order to avoid repeating arguments already expressed in [2] relative to the determination of the tool profile, from now on we will refer to [2] as regards the method, the common nomenclature and some figures.

In this case as well, we will introduce three reference systems equal to those used in [2] for convenience. The reference system S_f is rigidly connected to the machine tool frame.

The reference system S_s represents a reference rigidly connected to the screw rotor, performing a screw motion relative to the fixed reference, along the common axis $z_f \equiv z_s$. In the general instant t, the origin O_s will be shifted relative to O_f of $p\psi$, while the axes x_s and y_s make the angle ψ with the corresponding axes x_f and y_f [2].

The reference system S_c is rigidly connected to the tool. The distance of the milling cutter center O_c from the axis $z_f \equiv z_s$, indicated with e_c, is one of the most important cut parameters, along with the angle γ_c, which is the tool setting angle relative to the fixed reference system.

We use the notation $\mathbf{M}_{ab}$ for the transformation matrix from the reference system S_b to S_a. Refer to [2] for the analytical expressions of matrixes $\mathbf{M}_{cf}$ and $\mathbf{M}_{fs}$.

3. Tool Sharpening

In chapter 2 we saw that the milling cutter has eccentric relieved teeth. The sharpening action reduces the milling cutter diameter; therefore it becomes necessary to modify the distance e_c to maintain constant the inner radius of the rotor.

The topic of the following paragraphs is the proof that the diameter variation produces a different helicoidal shape for the screw rotor which is different from the theoretical shape.

3.1. CONTACT LINE BETWEEN SCREW ROTOR AND TOOL

The method that permits us to obtain the design of the tool shape is discussed in detail in [2] and here it is possible only to recall some facts. Now it is inferred that the profile of the tool is given and the analytical components of the vector $\mathbf{r}_c^{tool}$ which represent it are known.

In paper [2] we showed that equation $f(u_s, \vartheta_s) = 0$, which is the equation of meshing for the screw rotors, has only one solution, so theoretically it is possible to consider the surface parameter ϑ_s as a function of u_s. Therefore the section of the tool becomes a function of the parameter u_s only. The surface of revolution Σ_c^{tool} which represents the tool becomes function of the two surface parameters u_s and ϑ_c, related to the generation of the surface of revolution. We have also demonstrated in [2] that the functions obtained are continuous and derivable in their definition sets.

To calculate the effect of sharpening we introduce the parameter δ that represents the reduction of the milling cutter radius. In the following numerical examples, δ will be equal to 2 mm which corresponds to a milling cutter close to the end of its life-cycle. The other parameters in all the numerical examples are: r = 12 mm, r_e = 20 mm, a = 68 mm, γ = 45°, γ_c = 48°3′, e_c = (50 + r) mm for the central screw rotor and e_c = (50 + r_i) mm for the idler.

Thus the sharpened tool section and the surface of revolution that models it are respectively given by

$$\begin{cases} x_c^{sct-shr}\left(u_s\right) = -\sqrt{x_c^2\left(u_s, \vartheta_s\left(u_s\right)\right) + y_c^2\left(u_s, \vartheta_s\left(u_s\right)\right)} + \delta \\ z_c^{sct-shr}\left(u_s\right) = z_c\left(u_s, \vartheta_s\left(u_s\right)\right) \end{cases}, \tag{1}$$

$$\mathbf{r}_c^{shr}\left(u_s, \vartheta_c\right) = x_c^{sct-shr}\left(u_s\right)\cos\vartheta_c\,\mathbf{i}_c + x_c^{sct-shr}\left(u_s\right)\sin\vartheta_c\,\mathbf{j}_c + z_c^{sct-shr}\left(u_s\right)\mathbf{k}_c \tag{2}$$

where the surface coordinates $u_s \in \Xi'$ and $\vartheta_c \in [-\pi, \pi]$ determine the definition sets A_i.

So far we have analyzed the problem only from the analytical point of view. Now, if we consider a numerical case, we have to observe that an explicit function to express the radial cutter section - even if Dini's theorem guarantees its theoretical existence - is not available. To solve this problem, we have to introduce an interpolating function that represents the function $\vartheta_s = \vartheta_s(u_s)$ starting from the equation of meshing $f(u_s, \vartheta_s) = 0$.

We vary the value of u_s between its extreme values with a reduced step and numerically solved the equation for ϑ_s. So we obtain a set of couples of values (u_s, ϑ_s). Then we use a cubic polynomial curve to fit the data points. The software used can also treat this interpolating function as an approximate function and can perform all the operations possible for pure functions on the approximate function, such as the calculation of their derivatives, if they exist (as in this present case).

Since all the functions in equation (2) are at least C^1(A) for the considerations expressed in [2] and up to this point, the normal exists and is obtainable at every point for the sharpened tool surface:

$$\mathbf{N}_c = \frac{\partial \mathbf{r}_c^{shr}}{\partial u_s} \times \frac{\partial \mathbf{r}_c^{shr}}{\partial \vartheta_c} = N_{xc}\left(u_s, \vartheta_c\right)\mathbf{i}_c + N_{yc}\left(u_s, \vartheta_c\right)\mathbf{j}_c + N_{zc}\left(u_s, \vartheta_c\right)\mathbf{k}_c \ . \tag{3}$$

Obviously, the derivatives in (3) exist only theoretically and it is not possible to explicit them, since it is not yet possible to explicit $\vartheta_s = \vartheta_s(u_s)$. Practically speaking the derivatives in (3) are numerically calculated starting from the approximate functions introduced before and from now on numerical methods, with the use of cubic polynomial functions, will always be used to explicit theoretical analytical expressions.

For the determination of the equation of meshing, we refer to Litvin's theory [6]. The equation is given by a null scalar product of the normal to the surface and the tool velocity relative to the screw rotor. It is easy to explain this fact: the null scalar product means that the normal to the surface is orthogonal to the velocity, and this happens only at the point of cut. Considering the vectors, we have

$$\mathbf{N}_c \cdot \mathbf{v}_c^{(cs)} = 0 \ . \tag{4}$$

To determine $\mathbf{v}_c^{(cs)}$, we consider the milling cutter held at rest, when the tool is modeled as a surface of revolution, so we have

$$\mathbf{v}_c^{(cs)} = \mathbf{v}_c^{(c)} - \mathbf{v}_c^{(s)} = -\mathbf{v}_c^{(s)} \ . \tag{5}$$

Since during the machining the rotor has a screw motion along the z_s axis characterized by an angular velocity $\boldsymbol{\omega}^{(s)}$ and translational velocity $p\,\boldsymbol{\omega}^{(s)}$, we have

$$\mathbf{v}_c^{(s)} = \left(\boldsymbol{\omega}_c^{(s)} \times \mathbf{r}_c^{shr}\right) + \left(-e_c\mathbf{i} \times \boldsymbol{\omega}_c^{(s)}\right) + p\,\boldsymbol{\omega}_c^{(s)} \text{ , with } p = \frac{a}{2\pi}. \tag{6}$$

To obtain the screw rotor angular velocity $\boldsymbol{\omega}^{(s)}$ in the S_c reference system, we use the rotational submatrixes $\mathbf{L}_{cf}$ and $\mathbf{L}_{fs}$ of the transformation matrixes $\mathbf{M}_{cf}$ and $\mathbf{M}_{fs}$, considering that $\psi = 0$

$$\boldsymbol{\omega}_c^{(s)} = \mathbf{L}_{cf}\mathbf{L}_{fs}\boldsymbol{\omega}_s^{(s)} = \begin{bmatrix} 1 & 0 & 0 \\ 0 & \cos\gamma_c & \sin\gamma_c \\ 0 & -\sin\gamma_c & \cos\gamma_c \end{bmatrix}\begin{bmatrix} 0 \\ 0 \\ \omega^{(s)} \end{bmatrix} = \omega^{(s)}\begin{bmatrix} 0 \\ \sin\gamma_c \\ \cos\gamma_c \end{bmatrix}. \tag{7}$$

After the substitution of (7) in (6), we have

$$\mathbf{v}_c^{(cs)} = -\omega^{(s)}\begin{bmatrix} z_c^{shr}\sin\gamma_c - y_c^{shr}\cos\gamma_c \\ \left(x_c^{shr} + e_c\right)\cos\gamma_c + p\sin\gamma_c \\ -\left(x_c^{shr} + e_c\right)\sin\gamma_c + p\cos\gamma_c \end{bmatrix}. \tag{8}$$

If we calculate the scalar product (4) and simplify, we obtain the equation of meshing for the tools:

$$g\left(u_s, \vartheta_c\right) = \sin\gamma_c\, z_c^{shr}\, N_{xc} + \left(e_c\cos\gamma_c + p\sin\gamma_c\right)N_{yc} + \left[p\cos\gamma_c - \sin\gamma_c\left(x_c^{shr} + e_c\right)\right]N_{zc} = 0\ . \tag{9}$$

The couples of values $\left(\overline{u}_s, \overline{\vartheta}_c\right)$, which satisfy equation (9), state the solution locus Θ. By using the equation of meshing, the contact line Γ' on the sharpened tool is determined by the equation

$$\Gamma_c' \begin{cases} \mathbf{r}_c^{shr} = \mathbf{r}_c^{shr}\left(u_s, \vartheta_c\right) \\ g\left(u_s, \vartheta_c\right) = 0 \end{cases}. \tag{10}$$

Then it is possible to refer Γ' in the screw rotor reference system S_s with equation (11) where $\psi = 0$. By varying ψ in equation (11), the envelope is generated by a screw motion along the z_s axis and the surface Σ_s' of the screw rotor made by the sharpened tool is determined. The method introduced here could also be used to determine the surface enveloped by a generic tool, whose geometry $\mathbf{r}_c$ is known. Note that matrix $\mathbf{M}_{fc}{}^{shr}$ differs from $\mathbf{M}_{fc}$ given in [2] since we have to consider the reduction of the distance from O_c to z_s due to the reduction δ of the milling cutter radius.

$$\mathbf{r}_s^{shr} = \mathbf{M}_{sf}\mathbf{M}_{fc}^{shr}\mathbf{r}_c^{shr}\left(\overline{u}_s, \overline{\vartheta}_c\right) \text{ with } \left(\overline{u}_s, \overline{\vartheta}_c\right) \in \Theta\,, \tag{11}$$

$$\mathbf{M}_{fc}^{shr} = \begin{bmatrix} 1 & 0 & 0 & e_c - \delta \\ 0 & \cos\gamma_c & -\sin\gamma_c & 0 \\ 0 & \sin\gamma_c & \cos\gamma_c & 0 \\ 0 & 0 & 0 & 1 \end{bmatrix}. \tag{12}$$

Figure 2 shows the comparison between the contact lines of the theoretical tool and the sharpened tool which are both projected onto the theoretical screw rotor. The evaluation of the difference is reported in the next paragraph.

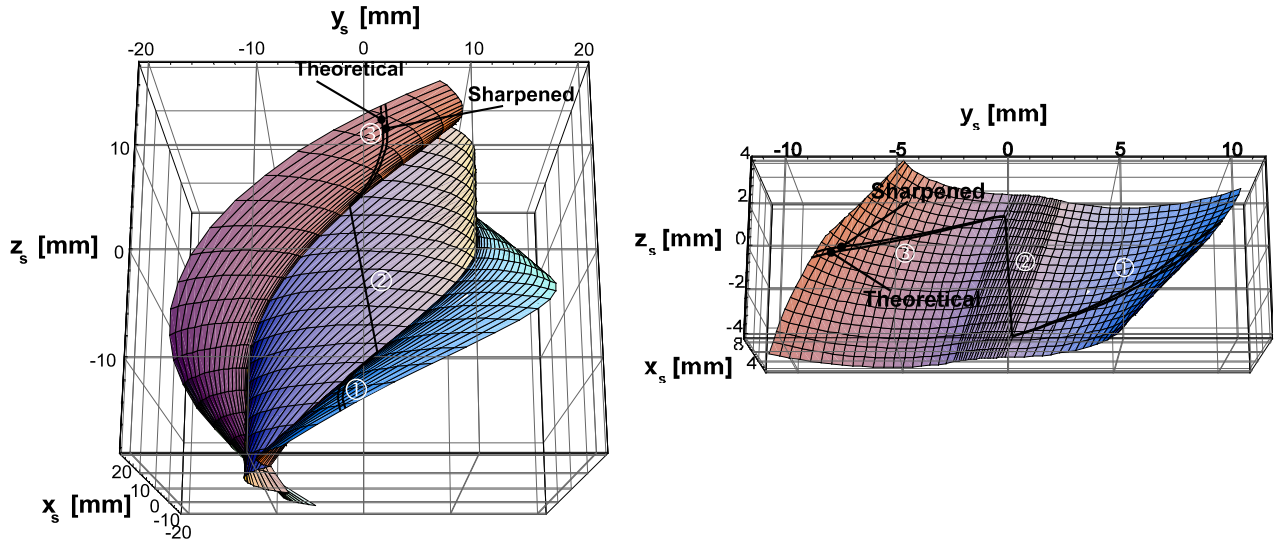

Figure 2 - Comparison between the contact lines of theoretical and sharpened tools: central screw rotor (left), idler screw rotor (right).

3.2. COMPARISON BETWEEN THEORETICAL AND SHARPENED TOOLS

The difference between the contact lines of figure 2 can be evaluated by projecting both lines onto the planes $x_s y_s$, $y_s z_s$ and $x_s z_s$, determined by the axes in the reference systems S_s of the screw rotors. In figure 3 the theoretical contact line for the central screw is plotted in a white solid line, while the line corresponding to the sharpened tool is plotted in a black dashed line. Similar results are obtained for the idler screw.

The numerical evaluation of the resulting deviation on the machined screw rotors can be made by calculating the distance $\varepsilon(\delta, \rho)$ between corresponding points, i.e. at the same distance ρ from the rotor rotation axis, of the theoretical line Γ_s and of the line relative to the sharpened tool Γ'_s.

$$\varepsilon(\delta,\rho)=\sqrt{\left(x_s-x_s^{shr}\right)^2+\left(y_s-y_s^{shr}\right)^2+\left(z_s-z_s^{shr}\right)^2}\ . \tag{13}$$

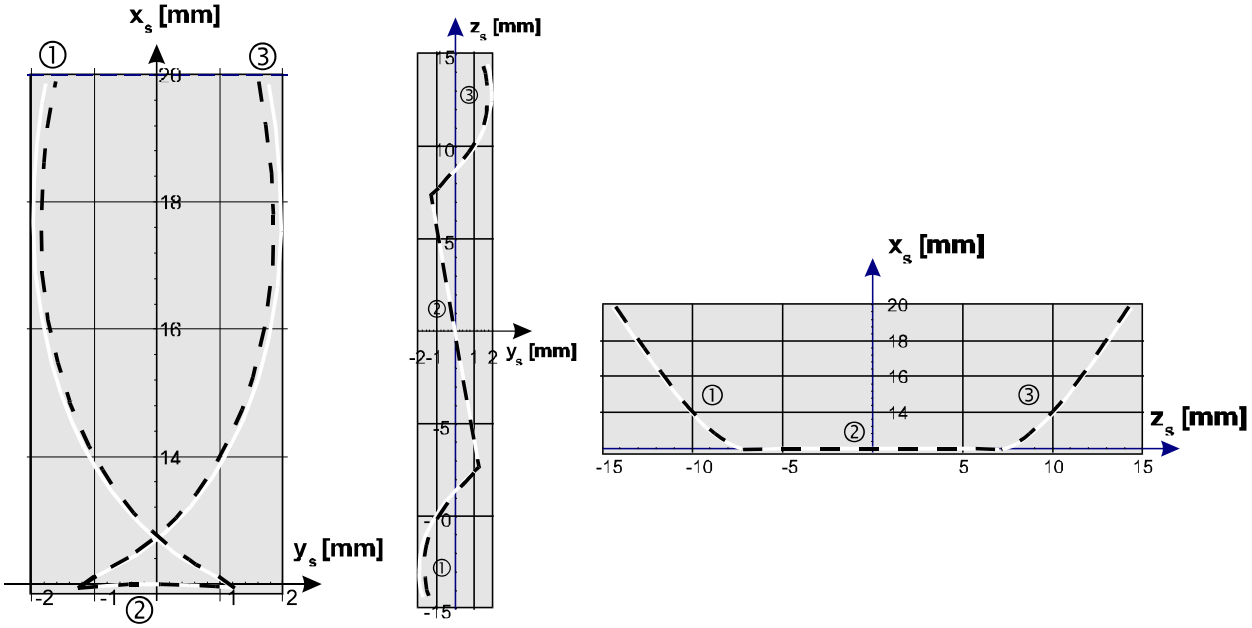

(a) (b) (c)

Figure 3 - Contact lines for the central screw rotor projected on $x_s y_s$ plane (a), $y_s z_s$ plane (b) and $x_s z_s$ plane (c).

In the diagrams of figure 4, deviation ε is plotted depending on the radial distance ρ of the points of the contact lines from the rotor axis, for the fixed value of δ. In both the diagrams, the vertical segment is relative to the deviation on the

cylindrical surface ② of figure 5, that is, at a constant distance from the rotation axis. Note that the deviation is null on the cylindrical surface at the point corresponding to the intersection of the surface and the tool axis x_c.

For the other flanks ① and ③ (see figure 5), the diagrams are superimposed due to the symmetry of the configuration. In the idler screw rotor case there is a distance where the deviation is null (C in figure 4), whereas for the central screw rotor the behavior is monotonic.

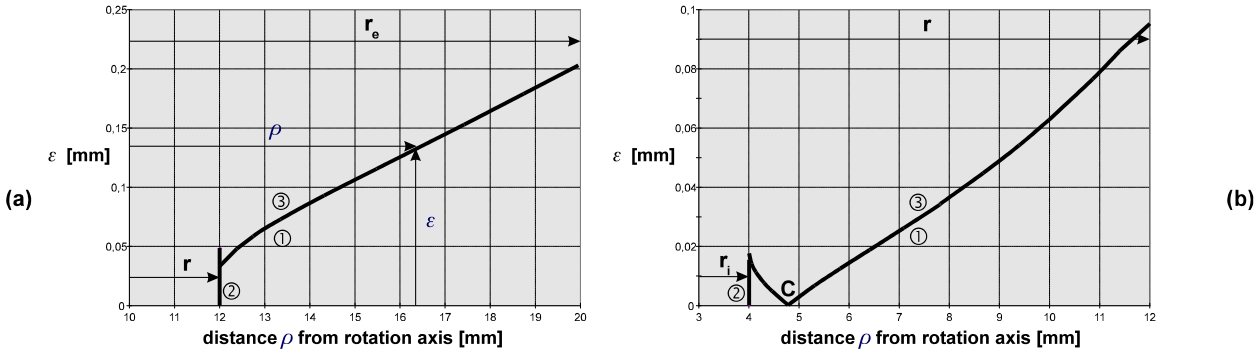

Figure 4 - Deviation due to sharpened tool: (a) central screw rotor, (b) idler screw rotor.

From the consideration of figures 3-4 and from the calculation of ε, we note that tool sharpening determines a variable deviation on the generated screw rotor depending on the flanks considered. In particular, the deviation is always lower for the idler screw rotor and extremely small for the cylindrical surfaces ② (see figure 4) in general. Finally, it can be observed that, for a given value δ of sharpening, the maximum error ε_{max} on the central screw rotor is about twice the maximum error on the idler screw rotor (about 0.2 mm vs. 0.1 mm as shown in figure 4). Besides, the flanks ① and ③ (see figure 5) tend to approach each other as shown in the following paragraph.

3.3. Comparison of the Profiles on a Screw Rotor Cross Section

Cutting the helicoids generated by equation (11) with plane $x_s y_s$, using the system

$$\begin{cases} \mathbf{r}_s^{shr} = x_s^{shr}\mathbf{i}_s + y_s^{shr}\mathbf{j}_s + z_s^{shr}\mathbf{k}_s \\ z_s^{shr}\left(\overline{u}_s, \overline{\vartheta}_c, \psi\right) = 0 \end{cases} \tag{14}$$

we obtain the relation between the parameters (not independent) $\left(\overline{u}_s, \overline{\vartheta}_c\right)$ and ψ. Those parameters which were introduced in the first equation of system (14), permit us to determine the cross sections of the screw rotors generated by sharpened tools. When these profiles (dashed lines in figure 5) are compared with those of theoretical screw rotors (solid line in figure 5), note that the effect of the sharpening determines an enlargement of the worm of the central screw rotor and a restriction of the vane of the idler screw rotor. This may cause the interference of the screw rotors and lead to the necessity for an adequate break-in to achieve correct meshing conditions.

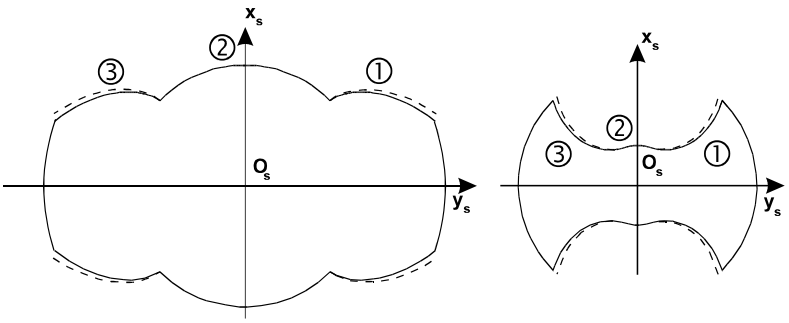

Figure 5 - Comparison of the profiles on a cross section: (a) central screw rotor, (b) idler screw rotor.

4. Proposed Solutions for Deviation Reduction

4.1. Variation of the Tool Setting Angle

Now we will see if it is possible to reduce the deviations by modifying the tool setting angle γ_c. Due to the nature of the problem that involves implicit functions such as *f* and *g*, a numerical method was used to simulate many practical cases. The results show that this variation cannot completely prevent the deviation. However it is possible to reduce it if we state the problem in this form: the search for angle $\tilde{\gamma}_c$ that minimizes the sum of the errors $\varepsilon_\Gamma(\delta, \rho)$ along the line Γ, that is

$$\min_{\tilde{\gamma}_c} \int_\Gamma \varepsilon(\delta, \rho)\, d\Gamma \quad . \tag{15}$$

The solution of this minimization procedure necessitate a long numerical analysis that has not been considered in this paper. However a quantitative evaluation has been done on small variations of the setting angle of some primes. In the case of figure 6, an increase of 6′ of the setting angle for the central screw rotor and a reduction of 12′ for the idler screw rotor can limit, but obviously not delete, the deviation. In particular, in this case it is possible to reduce the maximum deviation for both rotors. In figure 6 the white dashed line represents the deviations with the tool sharpened and the setting angle changed. The black solid line is the deviation due only to the sharpening equal to figure 4.

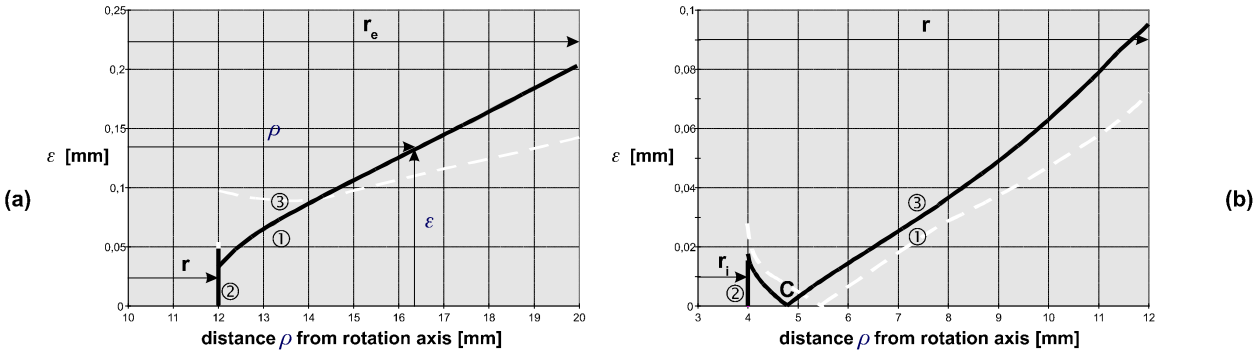

Figure 6 - Contact lines on $x_s y_s$ with different setting angle γ_c: central screw rotor (left), idler screw rotor (right).

4.2. Variable Profile Tools

From a theoretical point of view a possibility exists of eliminating the deviations due to the sharpening, by using a tool with a variable cutter profile. This is a tool (see figure 7) whose cutter section varies in function of the sharpening. Its design is made possible by varying the parameter e_c in function of δ and calculating each correct theoretical section by following the procedure introduced in [2].

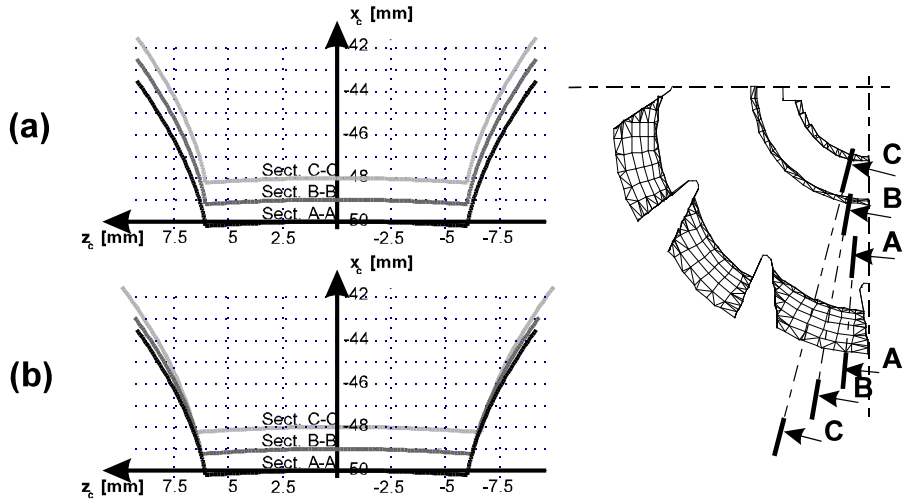

Figure 7 - Comparison between constant (a) and variable (b) profile tool.

4.3. DISK GRINDING WHEELS

Another possible solution is the use of disk grinding wheels which are shaped to obtain the exact surface of revolution depending on the real dimension of the grinding wheel when sharpened. The use of grinding wheels can delete the deviations and shaped milling cutters can be used only in the preliminary roughing phase. Since the grinding wheel shape must be periodically controlled and modified, a suitable technology must be available too.

5. Conclusions

In this paper we have considered the particular aspect of the machining of screw pump rotors that uses milling cutters. A mathematical model has been introduced which, on one hand, permits us to determine the surface enveloped by a tool. If the tool is new, the surface enveloped guarantees the correct kinematics.

On the other hand, the model permits us to determine the deviation introduced in the machining when the tool geometry changes due to the sharpening of the milling cutter.

Finally, we have introduced a method for reducing deviations by varying the setting angle of the milling cutter after sharpening, and two alternatives for eliminating deviations completely and we have illustrated their characteristics.

Acknowledgments

The research has been done thanks to a contribution of M.U.R.S.T. *ex - quota 40%*.

References

1. Mimmi, G., Pennacchi, P., 1995, 'Design of three-screw positive displacement rotary pumps', proceedings of *Contact Mechanics II-Computational Techniques*, 11-13 july 1995, Ferrara, Italy;
2. Mimmi, G., Pennacchi, P., 'Determination of Tool Profile for the Milling of Three Screw Pump Rotor', to be published on *Meccanica*, 1997;
3. ISO 3855, Milling cutters - Nomenclature, 1977;
4. Micheletti, G.F., *Tecnologia Meccanica*, vol.2, 2 ed., UTET, Torino, 1979;
5. Bruins, D.H., Dräger, H.J., *Utensili e Macchine Utensili ad Asportazione di Truciolo*, vol.1, Tecniche Nuove, Milano, 1981;
6. Litvin, F.L., *Gear Geometry and Applied Theory*, Prentice Hall, Englewood Cliffs, NJ, 1994.